



Gold(I) complexes with thiosemicarbazones: Cytotoxicity against human tumor cell lines and inhibition of thioredoxin reductase activity

Josane A. Lessa^a, Juliana C. Guerra^b, Luana F. de Miranda^b, Carla F.D. Romeiro^b, Jeferson G. Da Silva^a, Isolda C. Mendes^c, Nivaldo L. Speziali^d, Elaine M. Souza-Fagundes^b, Heloisa Beraldo^{a,*}

^a Departamento de Química, Universidade Federal de Minas Gerais, 31270-901, Belo Horizonte, MG, Brazil

^b Departamento de Fisiologia, Universidade Federal de Minas Gerais, 31270-901, Belo Horizonte, MG, Brazil

^c Escola de Belas Artes, Departamento de Artes Plásticas, Universidade Federal de Minas Gerais, 31270-901, Belo Horizonte, MG, Brazil

^d Departamento de Física, Universidade Federal de Minas Gerais, 31270-901, Belo Horizonte, MG, Brazil

ARTICLE INFO

Article history:

Received 1 June 2011

Received in revised form 19 August 2011

Accepted 2 September 2011

Available online 10 September 2011

Keywords:

Gold(I) complexes
Thiosemicarbazones
Cytotoxic activity
Thioredoxin reductase

ABSTRACT

Complexes [Au(H₂Ac₄DH)Cl]·MeOH (**1**) [Au(H₂Ac₄Me)Cl]Cl (**2**) [Au(H₂Ac₄Ph)Cl]Cl·2H₂O (**3**) and [Au(H₂Bz₄Ph)Cl]Cl (**4**) were obtained with 2-acetylpyridine thiosemicarbazone (H₂Ac₄DH), its *N*(4)-methyl (H₂Ac₄Me) and *N*(4)-phenyl (H₂Ac₄Ph) derivatives, as well as with *N*(4)-phenyl 2-benzoylpyridine thiosemicarbazone (H₂Bz₄Ph). The compounds were cytotoxic to Jurkat (immortalized line of T lymphocyte), HL-60 (acute myeloid leukemia), MCF-7 (human breast adenocarcinoma) and HCT-116 (colorectal carcinoma) tumor cell lines. Jurkat and HL-60 cells were more sensitive than MCF-7 and HCT-116 cells. Upon coordinating to the gold(I) metal centers in complexes (**2**) and (**4**), the cytotoxic activity of the H₂Ac₄Me and H₂Bz₄Ph ligands increased against the HL-60 and Jurkat tumor cell lines. **2** was more active than auranofin against both leukemia cells. Most of the studied compounds were less toxic than auranofin to peripheral blood mononuclear cells (PBMC). All compounds induced DNA fragmentation in HL-60 and Jurkat cells indicating their pro-apoptotic potential. Complex (**2**) strongly inhibited the activity of thioredoxin reductase (TrxR), which suggests inhibition of TrxR to be part of its mechanism of action.

© 2011 Elsevier Inc. All rights reserved.

1. Introduction

Cisplatin and the second generation complexes carboplatin and oxaliplatin are effective antitumor agents widely used in the treatment of testicular, ovarian, bladder and a variety of other solid tumors. Despite the clinical success of cisplatin, many tumors are intrinsically resistant to the drug, and tumors that are initially sensitive to cisplatin treatment often develop resistance during ongoing treatment regimens [1]. In addition, the compounds cause severe side effects which complicate their clinical application. Hence there is an increasing demand for novel metal-based-pharmaceuticals with a mode of action differing from that of the platinum generation of anticancer drugs [2].

Gold complexes have attracted significant attention as potential alternatives to cisplatin due to the fact that many gold(I) and gold(III) compounds have been found to inhibit tumor cell growth. Since gold compounds have been observed to interact with numerous intracellular protein targets (e.g., cathepsins, tyrosine phosphatases, cyclooxygenases, thioredoxin reductase, proteasomes, etc.), they have potential in treating cisplatin-resistant tumors [3]. The

anti-rheumatic drug triethylphosphinegold(I)tetraacetylthioglucose (auranofin) emerged as the lead compound for the class of anti-proliferative gold compounds [4].

The selenoenzyme thioredoxin reductase (TrxR) is considered as an emerging target for anticancer metallodrugs. Gold(I) and gold(III) complexes have shown promising anti-proliferative activity and demonstrated a significant potential as new anticancer agents. It has been suggested that the mechanism of action of these compounds involves targeting thioredoxin reductase [5]. TrxR is relevant for the proliferation of tumor tissues and its inhibition is related to the triggering of anti-mitochondrial effects [6].

Thiosemicarbazones are a class of compounds with wide pharmacological versatility, which exhibit antiviral, antitumor and antimicrobial activities [7]. The antitumor activity of $\alpha(N)$ -heterocyclic thiosemicarbazones has been attributed to their ability to inhibit ribonucleoside diphosphate reductase (RDR), a key enzyme in DNA biosynthesis, which catalyzes the synthesis of deoxyribonucleotides from their ribonucleotide precursors [8]. The antitumor properties of thiosemicarbazones [7,9] and their metal complexes [7,8,10–13] have been extensively investigated. Gold(I) [14] and gold(III) complexes [15] with thiosemicarbazones have been prepared and tested for their *in vitro* cytotoxic activity against tumor cell lines. However to our knowledge studies on gold complexes with thiosemicarbazones have not involved investigation on their interaction with TrxR.

* Corresponding author. Tel.: +55 31 34095740; fax: +55 31 34095700.
E-mail address: hberaldo@ufmg.br (H. Beraldo).

In the present work gold(I) complexes with 2-acetylpyridine thiosemicarbazone (H2Ac4DH), its *N*(4)-methyl (H2Ac4Me) and *N*(4)-phenyl (H2Ac4Ph) derivatives, as well as with *N*(4)-phenyl 2-benzoylpyridine thiosemicarbazone (H2Bz4Ph) (see Fig. 1) were tested for their cytotoxic activity against human leukemia and solid tumor cell lines. Since thioredoxin reductase (TrxR) is considered as the most relevant molecular target for gold compounds, inhibition of TrxR's activity by the studied gold(I) complexes was investigated.

2. Experimental

2.1. Physical measurements

All common chemicals were purchased from Aldrich and used without further purification. Partial elemental analyses were performed on a Perkin Elmer CHN 2400 analyzer. An YSI model 31 conductivity bridge was employed for molar conductivity measurements. Infrared spectra were recorded on a Perkin Elmer FT-IR Spectrum GX spectrometer using KBr plates (4000–400 cm^{-1}) and nujol mulls between CsI plates (400–170 cm^{-1}). NMR spectra were obtained with a Bruker AVANCE DPX 200 (200 MHz) spectrometer using $\text{CD}_3\text{OD}-d_4$ as the solvent and TMS as internal reference.

2.2. Synthesis of 2-acetylpyridine thiosemicarbazone (H2Ac4DH), its *N*(4)-methyl (H2Ac4Me) and *N*(4)-phenyl (H2Ac4Ph) derivatives and *N*(4)-phenyl 2-benzoylpyridine thiosemicarbazone (H2Bz4Ph)

All thiosemicarbazones were prepared as previously described [16].

2.3. Synthesis of the gold(I) complexes

The gold complexes were obtained by mixing a methanol/acetone (1:1) solution of the desired thiosemicarbazone (1 mmol) with hydrogen tetrachloroaurate(III) ($\text{HAuCl}_4 \cdot 3\text{H}_2\text{O}$) in 1:1 ligand-to-metal molar ratio at room temperature with stirring for 2 h (see Scheme 1). The resulting solids were filtered off then washed with acetone and dried *in vacuo*.

2.3.1. [(2-acetylpyridine thiosemicarbazone)chlorogold(I)], $[\text{Au}(\text{H}_2\text{Ac}_4\text{DH})\text{Cl}]\cdot\text{MeOH}$ (**1**)

Light-Brown solid. Anal. Calc. ($\text{C}_9\text{H}_{14}\text{ClN}_4\text{SOAu}$): C, 23.56; H, 3.08; N, 12.21%; Found: C, 23.84; H, 3.05; N, 12.07%. FW: 458.72 $\text{g}\cdot\text{mol}^{-1}$. IR (KBr, cm^{-1}): 3284 medium (m), 3240 m $\nu(\text{NH})$, 3100 $\nu(\text{OH})$, 1623 strong (s) $\nu(\text{C}=\text{N})$, 775 m $\nu(\text{C}=\text{S})$, 621 weak (w) $\rho(\text{py})$. IR (CsI/nujol, cm^{-1}): 348w $\nu(\text{Au}-\text{S})$, 330w $\nu(\text{Au}-\text{Cl})$. ^1H NMR [200 MHz, $\text{CD}_3\text{OD}-d_4$, δ (ppm), δ (ppm) free ligand in parenthesis]:

8.92 (8.56) [doublet (d), 1H, H6]; 8.46 (8.17) [d, 1H, H3]; 8.67 (7.82) [triplet (t), 1H, H4]; 8.07 (7.38) [t, 1H, H5]; 2.57 (2.40) [singlet (s), 3H, CH_3]. $\Lambda_{\text{M}} = 49.73 \Omega^{-1} \cdot \text{cm}^2 \cdot \text{mol}^{-1}$ in dimethylformamide (DMF). Yield 58%.

2.3.2. [(*N*(4)-methyl 2-acetylpyridinium thiosemicarbazone)chlorogold(I)] chloride, $[\text{Au}(\text{H}_2\text{Ac}_4\text{Me})\text{Cl}]\text{Cl}$ (**2**)

Rust colored solid. Anal. Calc. ($\text{C}_9\text{H}_{13}\text{Cl}_2\text{N}_4\text{SAu}$): C, 22.65; H, 2.75; N, 11.74%. Found: C, 22.91; H, 2.68; N, 11.51%. FW: 477.16 $\text{g}\cdot\text{mol}^{-1}$. IR (KBr, cm^{-1}): 3284 m $\nu(\text{NH})$, 2910 $\nu(\text{N}_{\text{py}}^+\text{H})$, 1623 $\nu(\text{C}=\text{N})$, 775 m $\nu(\text{C}=\text{S})$, 622w $\rho(\text{py})$. IR (CsI/nujol, cm^{-1}): 362w $\nu(\text{Au}-\text{S})$, 344w $\nu(\text{Au}-\text{Cl})$. ^1H NMR [200 MHz, $\text{CD}_3\text{OD}-d_4$, δ (ppm), δ (ppm) free ligand in parenthesis]: 9.00 (8.53) [d, 1H, H6]; 8.22 (8.17) [d, 1H, H3]; 8.47 (7.80) [t, 1H, H4]; 7.96 (7.35) [t, 1H, H5]; 3.15 (3.14) [s, 3H, CH_3]; 2.67 (2.36) [s, 3H, CH_3]. $\Lambda_{\text{M}} = 127.42 \Omega^{-1} \cdot \text{cm}^2 \cdot \text{mol}^{-1}$ in DMF. Yield 65%.

2.3.3. [(*N*(4)-phenyl 2-acetylpyridinium thiosemicarbazone)chlorogold(I)] chloride dihydrate, $[\text{Au}(\text{H}_2\text{Ac}_4\text{Ph})\text{Cl}]\text{Cl} \cdot 2\text{H}_2\text{O}$ (**3**)

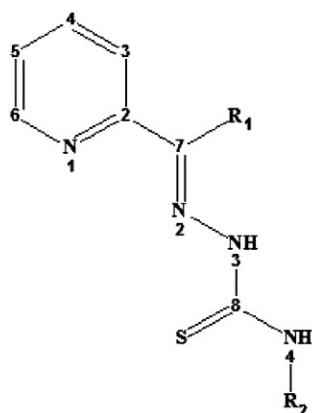
Dark red solid. Anal. Calc. ($\text{C}_{14}\text{H}_{19}\text{O}_2\text{Cl}_2\text{N}_4\text{SAu}$): C, 29.23; H, 3.33; N, 9.74%. Found: C, 29.36; H, 3.11; N, 9.54%. FW: 575.26 $\text{g}\cdot\text{mol}^{-1}$. IR (KBr, cm^{-1}): 3230 m $\nu(\text{NH})$, 2920 $\nu(\text{N}_{\text{py}}^+\text{H})$, 1619 s $\nu(\text{C}=\text{N})$, 797 m $\nu(\text{C}=\text{S})$, 602w $\rho(\text{py})$. IR (CsI/nujol, cm^{-1}): 370w $\nu(\text{Au}-\text{S})$, 363w $\nu(\text{Au}-\text{Cl})$. ^1H NMR [200 MHz, $\text{CD}_3\text{OD}-d_4$, δ (ppm), δ (ppm) free ligand in parenthesis]: 9.08 (8.60) [d, 1H, H6]; 8.34 (8.20) [d, 1H, H3]; 8.55 (7.88) [t, 1H, H4]; 8.04 (7.38) [t, 1H, H5]; 2.79 (2.47) [s, 3H, CH_3]. $\Lambda_{\text{M}} = 90.29 \Omega^{-1} \cdot \text{cm}^2 \cdot \text{mol}^{-1}$ in DMF. Yield 85%.

2.3.4. [(*N*(4)-phenyl 2-benzoylpyridinium thiosemicarbazone)chlorogold(I)] chloride $[\text{Au}(\text{H}_2\text{Bz}_4\text{Ph})\text{Cl}]\text{Cl}$ (**4**)

Dark red solid. Anal. Calc. ($\text{C}_{19}\text{H}_{17}\text{Cl}_2\text{N}_4\text{SAu}$): C, 37.95; H, 2.85; N, 9.32%; Found: C, 37.73; H, 2.74; N, 9.31%. FW: 601.30 $\text{g}\cdot\text{mol}^{-1}$. IR (KBr, cm^{-1}): 3226 m $\nu(\text{NH})$, 2682 $\nu(\text{N}_{\text{py}}^+\text{H})$, 1618 s $\nu(\text{C}=\text{N})$, 778 m $\nu(\text{C}=\text{S})$, 615w $\rho(\text{py})$. IR (CsI/nujol, cm^{-1}): 369w $\nu(\text{Au}-\text{S})$, 351w $\nu(\text{Au}-\text{Cl})$. ^1H NMR [200 MHz, $\text{CD}_3\text{OD}-d_4$, δ (ppm), δ (ppm) free ligand in parenthesis]: 9.15 (8.65, E; 8.84, Z) [d, 1H, H6]; 7.76 (7.75–7.50, E, Z) [d, 1H, H3]; 8.41 (7.83, E; 7.95, Z) [t, 1H, H4]; 8.02 (7.28–7.12, E, Z) [t, 1H, H5] [s, 1H, H15]. $\Lambda_{\text{M}} = 111.95 \Omega^{-1} \cdot \text{cm}^2 \cdot \text{mol}^{-1}$ in DMF. Yield 60%.

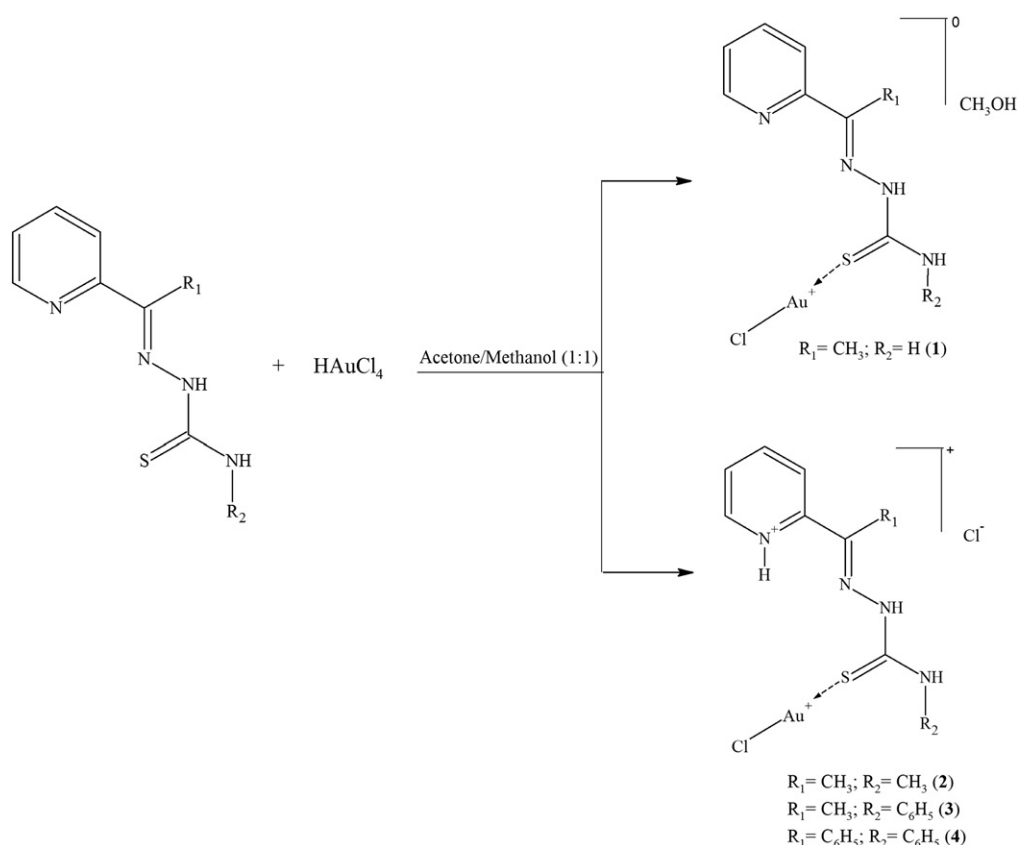
2.4. X-ray crystallography

Crystals of $[\text{Au}(\text{H}_2\text{Ac}_4\text{DH})\text{Cl}]\text{Cl} \cdot \text{H}_2\text{O}$ (**1a**) and $[\text{Au}(\text{H}_2\text{Bz}_4\text{Ph})\text{Cl}]\text{Cl}$ (**4**) were isolated from the filtrate in the syntheses of complexes (**1**) and (**4**). Structures of **1a** and **4** were determined using single-crystal X-ray diffraction. The measurements were carried out on an Oxford-GEMINI diffractometer with graphite monochromated Mo-K



Thiosemicarbazone	R ₁	R ₂
H2Ac4DH	CH ₃	H
H2Ac4Me	CH ₃	CH ₃
H2Ac4Ph	CH ₃	C ₆ H ₅
H2Bz4Ph	C ₆ H ₅	C ₆ H ₅

Fig. 1. Generic representation for pyridine-derived thiosemicarbazones.



Scheme 1. Synthesis of complexes (1–4).

radiation ($\lambda = 0.71073 \text{ \AA}$) at 293(2) K. Data collection, cell refinement, and data reduction were performed using the CRYCALISPRO software [17,18]. A semi-empirical absorption correction method was applied [17,18]. The structures were solved using SHELXS-97 [19] and refined using the SHELXL-97 software [19]. Positional and anisotropic atomic displacement parameters were refined for all non-hydrogen atoms. Hydrogen atoms were placed geometrically and the positional parameters were refined using a riding model, with exception of the water molecule of **1a**; in this case, the hydrogen atom positions were refined using the 'DFIX' command, with a separation of 1.38 \AA , the HO distance constrained to 0.82 \AA and $U_{\text{iso}} = 1.5U_{\text{eq}}(\text{O})$. Crystal data, data-collection parameters, and structure-refinement results are summarized in Table 1.

2.5. Cytotoxic activity

2.5.1. Materials

Cisplatin, auranofin, (3-(4,5-Dimethylthiazol-2-yl)-2,5-diphenyl-tetrazolium bromide) (MTT), RPMI-1460, L-glutamine were purchased from Sigma, and Antibiotic/Antimycotic Solution and fetal calf serum were purchased from Gibco (Grand Island, NY).

2.5.2. Cell lines

Jurkat (human immortalized line of T lymphocyte), HL-60 (wild type human promyelocytic leukemia), MCF-7 (human breast adenocarcinoma) and HCT-116 (human colorectal carcinoma) cell lines were kindly given by Dr. Gustavo Amarante-Mendes (São Paulo University, Brazil). All lineages were maintained in the logarithmic phase of growth in RPMI 1640 medium supplemented with 100 U.mL^{-1} penicillin and $100 \mu\text{g.mL}^{-1}$ streptomycin (GIBCO BRL, Grand Island, NY) enriched with 2 mM of L-glutamine and 10% of fetal bovine serum. All cultures were maintained at 37°C in a humidified

Table 1

Crystal data and structure refinement for $[\text{Au}(\text{H}_2\text{Ac4DH})\text{Cl}]\text{Cl}\cdot\text{H}_2\text{O}$ (**1a**) and $[\text{Au}(\text{H}_2\text{Bz4Ph})\text{Cl}]\text{Cl}$ (**4**).

Compound	$[\text{Au}(\text{H}_2\text{Ac4DH})\text{Cl}]\text{Cl}\cdot\text{H}_2\text{O}$ (1a)	$[\text{Au}(\text{H}_2\text{Bz4Ph})\text{Cl}]\text{Cl}$ (4)
Empirical formula	$\text{C}_8\text{H}_{13}\text{AuCl}_2\text{N}_4\text{OS}$	$\text{C}_{19}\text{H}_{17}\text{Cl}_2\text{N}_4\text{SAu}$
Formula weight	481.15	601.29
Crystal system	Monoclinic	Monoclinic
Space group	P 21/n	P 21/c
Wavelength, \AA	0.71073	0.71073
Unit cell dimensions	a, \AA 8.2261(2) b, \AA 15.5254(3) c, \AA 10.7882(3) α , $^\circ$ 90 β , $^\circ$ 96.523(2) γ , $^\circ$ 90	13.2675(2) 6.8000(2) 22.9706(5) 90 93.175(2) 90
Volume, \AA^3	1368.88(6)	2069.20(8)
Z/density calc., Mg/m^3	4 / 2.335	4 / 1.930
Absorption coefficient, mm^{-1}	11.279	7.480
F(000)	904	1152
Crystal size, mm	$0.38 \times 0.12 \times 0.06$	$0.24 \times 0.16 \times 0.10$
θ range for data coll., $^\circ$	2.81 to 29.52	3.08 to 29.51
Index range	$-10 \leq h \leq 10$ $-19 \leq k \leq 19$ $-13 \leq l \leq 13$	$-18 \leq h \leq 16$ $-7 \leq k \leq 9$ $-28 \leq l \leq 24$
Completeness	99.9 (to $2\theta = 26.37^\circ$)	86.4 (to 29.51°)
Refinement method	Full-matrix least-squares on F^2	Full-matrix least-squares on F^2
Extinction coefficient	None	0.00055(6)
Goodness-of-fit on F^2	0.986	0.887
Reflec. collect./unique $[R_{\text{int}}]$	16341 / 2796 $[R(\text{int}) = 0.0881]$	11961 / 4986 $[R(\text{int}) = 0.0214]$
Data/restraints/parameters	2796 / 3 / 161	4986 / 0 / 244
Final R indices $[I > 2\sigma(I)]$	$R_1 = 0.0282$ $wR_2 = 0.0654$	$R_1 = 0.0238$ $wR_2 = 0.0417$
R indices (all data)	$R_1 = 0.0354$ $wR_2 = 0.0668$	$R_1 = 0.0412$ $wR_2 = 0.0434$
Larg. peak & hole, $\text{e} \text{ \AA}^{-3}$	0.577 and -0.969	0.631 and -0.832

incubator with 5% CO₂ and 95% air. The media were changed twice weekly and they were regularly examined.

2.5.3. Evaluation of the cytotoxic effect against human tumor cell lines

Jurkat and HCT-116 lineages were inoculated at 100,000 cells of per well, while HL-60 and MCF-7 were inoculated at 50,000 and 40,000 cells of per well, respectively. The plates were pre-incubated for 24 h at 37 °C to allow adaptation of cells prior to the addition of the test compounds. Freshly prepared solutions of the different compounds were tested at 10 μM. Subsequently, the plates were inoculated for 48 h in an atmosphere of 5% CO₂ and 100% relative humidity. Control groups included treatment with 0.1% DMF (negative control) and 10 μM of cisplatin and auranofin (positive controls). Cell viability was estimated by measuring the rate of mitochondrial reduction of MTT. All substances were dissolved in DMF prior to dilution.

Compounds that inhibited the proliferation in more than 50% were selected for determination of the half maximal inhibitory concentration (IC₅₀). IC₅₀ values were determined over a range of concentrations (100–0.01 μM). All compounds were tested in triplicate, in three independent experiments.

2.5.4. Evaluation of the cytotoxic effect against human peripheral blood mononuclear cells

The human peripheral blood mononuclear cells (PBMC) were separated according to the method described by Gazzinelli et al. [20]. In brief, PBMC samples were obtained through agreement with Minas Gerais Hematology and Hemotherapy Center Foundation – HEMOMINAS (protocol n° 105/2004) from healthy adult volunteers of both sexes by centrifugation of heparinized venous blood over Ficoll cushion (Sigma-Aldrich, St. Louis, MO). Mononuclear cells were collected from the interphase after Ficoll separation and washed three times in RPMI-1640 before further processing. The cells were washed and the cell density was adjusted to 2.5×10^6 cells.mL⁻¹. 100 μL of this suspension (250,000 cells) were added to 96-well plate and incubated for 24 h in the presence of 2.5 μg.mL⁻¹ of phytohemagglutinin (PHA) for stabilization. After this period, cells were incubated in the presence of different concentrations of selected compounds (from 100 to 0.00001 μM) for 48 h, at 37 °C in a humidified atmosphere containing 5% CO₂. The cells were maintained in culture medium containing RPMI (Sigma) supplemented with 5% normal human serum AB Rh+, previously inactivated, 2 mM L-glutamine and an antibiotic/anti-mycotic solution containing 1000 U/mL penicillin, 1000 μg/mL streptomycin and 25 μg/mL fungisone (GIBCO/BRL, Grand Island, NY) was added to control fungal and bacterial contamination.

All experiments were performed in triplicate using auranofin as positive control. We conducted a solvent control (DMF) at the same concentration of the tested samples (less than 0.5%). Proliferation and viability were evaluated by the MTT assay.

2.5.5. In vitro cell viability assay – MTT assay

The MTT assay is a standard colorimetric assay, in which mitochondrial activity is measured by splitting tetrazolium salts with mitochondrial dehydrogenases in viable cells only [21]. Briefly, after 4 h of the end of incubation of cells with different compounds, 20 μL of MTT solution (2.5 mg.mL⁻¹ in phosphate-buffered saline) were added to each well, the supernatant was removed and 200 μL of 0.04 M HCl in isopropyl alcohol were added to dissolve the formazan crystals. The optical densities (OD) were measured in a spectrophotometer at 570 nm. Controls included drug-containing medium (background) and drug-free complete medium. Drug-free complete medium was used as control (blank) and was treated in the same way as the drug-containing media. Results were expressed as percentage of cell proliferation, comparing with 0.1% DMF control and were calculated as follows: viability (%) = (mean OD treated – mean OD background) / mean OD untreated cultured, i.e. 0.1% DMF – mean OD blank wells) × 100. Interactions of compounds and media were estimated on the basis of the variations

between drug-containing medium and drug-free medium to escape from false-positive or false-negative [22].

2.5.6. DNA fragmentation assay

The sub-diploid DNA content was determined for the quantification of cellular DNA fragmentation, which is characteristic of apoptosis. This experiment was used as a predictive method of the proapoptotic potential of the compounds. The sub-diploid DNA content was evaluated in HL-60, Jurkat, MCF-7 and HCT cells subjected to different treatments with selected compounds, according to the method described by Nicoletti et al. [23]. For this study, 200,000 cells in suspension treated or not with compounds were centrifuged for 5 min at 200 g, 4 °C. After centrifugation cells were re-suspended in hypotonic fluorochrome solution-HFS (50 μg.mL⁻¹ propidium iodide – PI (Sigma), 0.1% sodium citrate (Sigma) and 0.1% Triton X-100 (Sigma)). The samples in HFS were incubated at 8 °C for 4–8 h and immediately taken to the flow cytometer.

Incubation of cells with a hypotonic fluorochrome solution (HFS) leads to the weakening of the cell membrane by the action of Triton-X100 and hypotonic shock causes its lysis. The nuclear material becomes accessible to PI, which will intercalate in nuclear DNA. Normal cells have DNA content equal to 2n or 4n, depending on the phase of the cell cycle. In apoptotic cells the DNA content is lower than 2n, because the fragments of small molecular weight leave the inner core, which is the sub-diploid phase. The sub-diploid DNA content was determined by the CellQuest program (Becton Dickinson).

2.5.7. Statistical analysis

All experiments were performed in at least three replicates per compound and results shown are the average of three independent experiments. Data are represented as mean ± SEM. Significance was tested by the Student's t-test.

2.6. Studies of interactions with supercoiled plasmid DNA

Agarose gel electrophoresis was carried out to identify the modifications resulting from the interaction of complexes with DNA. Thus, 100 ng of purified pGEM®-T plasmid DNA (Promega-USA) were incubated with compounds (H2Ac4Me, **2**, HgCl₂ and auranofin) at the same concentration (100 μM) in Tris-HCl buffer (NaCl 50 mM, Tris-HCl 5 mM, pH 7.2). The mixture was incubated at 37 °C for 24 h. Thereafter, the reactions were quenched by adding 5 μL of a loading buffer solution (50 mM Tris, pH 7.2, 0.01% bromophenol blue, 50% glycerol, and 250 mM EDTA). The samples were analyzed by 1% agarose gel electrophoresis in 0.5 X TBE buffer for 1 h at 75 mV. The gel was stained after electrophoresis in 0.5 X TBE buffer with 2.5 μg mL⁻¹ ethidium bromide for 15 min and visualized by UV light.

2.7. Inhibition of thioredoxin reductase (TrxR) activity

Rat liver TrxR (Sigma) was used to determine TrxR inhibition by the compounds. The assay was performed according to the manufacturer's instructions (Sigma product information sheet T9698) and Ott and co-workers [24] with appropriate modifications. Initially, the TrxR rat liver solution was diluted with 1.0 M potassium phosphate buffer, pH 7.0. To 20 μL aliquots of this solution (each containing approximately 0.10 units of the enzyme) 20 μL of a solution of complex (**2**) in 5% DMF/potassium phosphate buffer pH 7.0 (in ten different concentrations in the 0.05–50.0 μM range) or vehicle without compound (control) were added, and the resulting solutions were incubated for 1 h at 37 °C with moderate shaking. For H2Ac4Me, HgCl₂ and auranofin the experiments were performed at 0.5, 5.0 and 10.0 μM in order to compare their inhibitory activities with that of complex (**2**). The solutions were transferred quantitatively to 96-well plates, and to each well 200 μL of reaction mixture (10 mL of

reaction mixture consisted of 1.0 mL of 1.0 M potassium phosphate buffer, pH 7.0, 0.20 mL of 500 mM EDTA solution pH 7.5, 0.80 mL of 63 mM dithiobisnitrobenzoic acid (DTNB) in ethanol, 0.10 mL of 20 mg/mL bovine serum albumin, 0.05 mL of 48 mM nicotinamide adenine dinucleotide phosphate (NADPH) and 7.85 mL of water) were added.

To correct for non-enzymatic product formation, 40 μ L of 2.5% DMF potassium phosphate buffer 1.0 M, pH 7.0, and 200 μ L of reaction mixture were processed simultaneously (blank). After proper mixing the formation of 5-thionitrobenzol (TNB) was monitored in a microplate reader (Thermo Scientific Multiskan® Spectrum) at 412 nm in 2 s intervals for 4 min. The absorbance of the blank was subtracted from that of the control and treated wells. The enzymatic activity was calculated as the maximum absorbance observed in 4 min in each well. The experiments were performed in triplicate. The EC_{50} value was calculated as the concentration of complex (2) decreasing the enzymatic activity by 50%.

3. Results and discussion

3.1. Formation of the gold(I) complexes

Microanalyses and molar conductivity data are compatible with the formation of gold(I) complexes $[Au(H_2Ac_4DH)Cl] \cdot MeOH$ (1) $[Au(H_2_2Ac_4Me)Cl]Cl$ (2) $[Au(H_2_2Ac_4Ph)Cl]Cl \cdot 2H_2O$ (3) and $[Au(H_2_2Bz_4Ph)Cl]Cl$ (4). In complex (1) a neutral thiosemicarbazone ligand (H_2Ac_4DH) is attached to the metal center together with a chloride. In 2–4 there is one positively charged thiosemicarbazone ($H_2_2Ac_4R$, R = methyl, phenyl; $H_2_2Bz_4Ph$) and one chloride as ligands and a chloride acts as counter ion, as confirmed by the crystal structure of 4 which reveals that the pyridine nitrogen is protonated (see Section 3.3).

Reduction of gold(III) to gold(I) took place in all cases, as observed for other gold complexes with thiosemicarbazones [25]. Reduction of gold(III) by the thiosemicarbazones could occur considering that these compounds exhibit reducing properties as previously shown by previous reports [26]. However, since we obtained the complexes in good yields reduction of gold(III) with oxidation of methanol could also take place. In complex (1) a crystallization methanol molecule is present as confirmed by its thermo-gravimetric curve which shows a weight loss of 7.3% (calcd 7.0%). In complex (3) two crystallization water molecules are present as shown by its thermo-gravimetric curve which reveals a weight loss of 6.1% (calcd. 6.3%). The presence

of solvation molecules in 1 and 3 was also corroborated by their infrared spectra (see Section 3.2).

3.2. Spectroscopic characterization

The $\nu(C=S)$ vibration observed at 802–755 cm^{-1} in the infrared spectra of the free thiosemicarbazones shifts to 797–775 cm^{-1} in the spectra of 1–4, indicating coordination of a thione sulfur [27]. A fairly strong and very broad absorption band observed at 2920–2682 cm^{-1} in the spectra of complexes (2–4) was attributed to the $\nu(N-H^+)$ stretching vibration of the pyridinium group [28]. Absorptions observed at 370–348 cm^{-1} were assigned to the $\nu(Au-S)$ vibration [14]. In addition, an absorption attributed to the $\nu(Au-Cl)$ vibration was observed at 363–330 cm^{-1} in the spectra of 1–4 [29]. A broad absorption at 3200–3100 cm^{-1} in the spectrum of complex (1) and at 3370 cm^{-1} in the spectrum of complex (3) was attributed to the $\nu(O-H)$ vibration.

Although all thiosemicarbazones and gold(I) complexes were soluble in $DMSO-d_6$ the complexes reacted with the solvent. Thus the NMR spectra of all studied compounds were recorded in methanol- d_4 .

The 1H resonances were assigned on the basis of chemical shifts and multiplicities. We did not obtain ^{13}C NMR spectra of 1–4 due to their low solubility in methanol- d_4 . Only one signal was observed for each hydrogen in the 1H NMR spectrum of all acetylpyridine-derived thiosemicarbazones, indicating the presence of only the *E* configurational isomer in solution [9]. The spectrum of H_2Bz_4Ph shows duplicated signals indicating the presence of the *Z* and *E* isomers in solution (50% each isomer). In complexes (1–4) the signals of all hydrogens undergo significant shifts in relation to their positions in the free bases (see Section 2.3). In the spectra of complexes (1–4) only one signal was observed for each hydrogen, suggesting the presence of only one isomer. The crystal structures of $[Au(H_2_2Ac_4DH)Cl]Cl \cdot H_2O$ (1a) and $[Au(H_2_2Bz_4Ph)Cl]Cl$ (4) reveal that the thiosemicarbazones adopt the *E* configuration (See Section 2.3).

3.3. X-ray crystallography

In complexes (1a) and (4) gold(I) is coordinated by the sulfur from the thiosemicarbazone together with a chloride ion in a distorted linear environment (see Fig. 2), which is typical of gold(I) complexes [14,30,31]. Other works report crystal structures of gold(I) complexes with thiosemicarbazones [14,30,31] which contain the metal center attached either to two sulfurs [30,31] or to a sulfur and

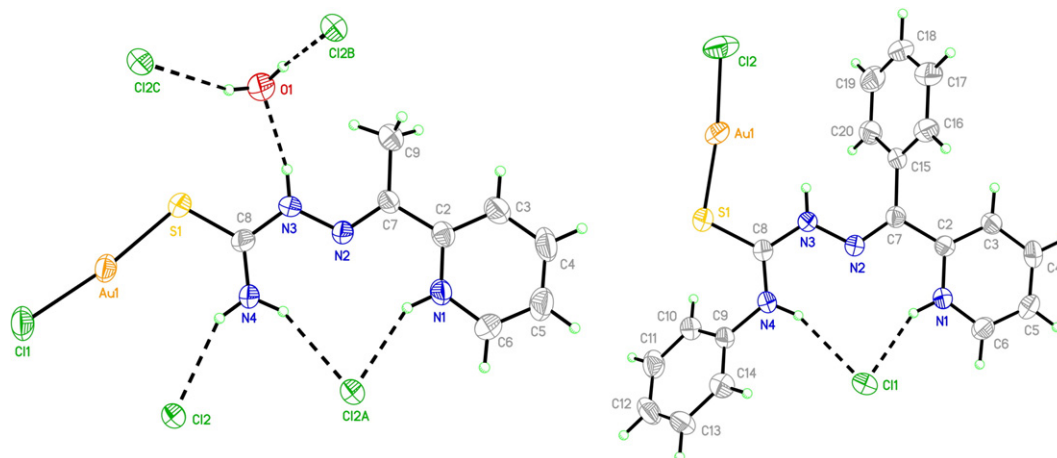


Fig. 2. Molecular plot of $[Au(H_2_2Ac_4DH)Cl]Cl \cdot H_2O$ (1a, left) and $[Au(H_2_2Bz_4Ph)Cl]Cl$ (4, right) showing the labeling scheme of the non-H atoms and their displacement ellipsoids at the 50% probability level. Intermolecular interactions via hydrogen bond are presented in dashes. In 1a, the Cl2A, Cl2B and Cl2C atoms were generated by symmetry transformations.

a phosphine [14]. To our knowledge this is the first report on complexes containing the gold center attached to a sulfur and a chloride as ligands.

The crystallographic data confirm reduction of gold(III) during the synthesis. In both complexes the thiosemicarbazone is protonated at the pyridine nitrogen. Thus, although complex (1) presents a neutral thiosemicarbazone in the powder, in **1a**, obtained from the filtrate, the thiosemicarbazone is protonated at the pyridine nitrogen, like in complexes (2–4), as a consequence of the presence of acidic hydrogen tetrachloroaurate in the reaction medium.

Lengthening of the S1–C8 bond from 1.681(3) Å in [H₂2Ac4DH]Cl (a thiosemicarbazone hydrochloride containing the pyridinium group) [32] to 1.712(5) Å in **1a** and from 1.663(2) Å in H2Bz4Ph [33] to 1.701(3) Å in **4**, together with the shortening of the N3–C8 bond from 1.371(3) Å in [H₂2Ac4DH]Cl [32] to 1.345(6) Å in **1a** and from 1.360(2) Å in H2Bz4Ph [33] to 1.345(3) Å in **4**, were noticed. The observed S1–C8 bond lengthening is compatible with coordination of a thione sulfur and is less than the lengthening observed upon coordination of thiosemicarbazones to gold(I) through a thiolate sulfur [34]. Selected bond lengths and angles are shown in Tables 2 and 3.

In **1a** and **4** the thiosemicarbazone adopts the *EE* conformation in relation to the C7=N2 and N3–C8 bonds. This conformation is the same as that observed for [H₂2Ac4DH]Cl [32]. In contrast, H2Bz4Ph presents *ZE* conformation [33]. In fact, the N1H...Cl and N4H...Cl hydrogen bonds in the structure of [H₂2Ac4DH]Cl were also observed for **1a** and **4** (See Table 4), suggesting that these hydrogen bonds favor the adoption of the *EE* conformation (See Table 4 and Fig. 2).

The N3C8S1Au1 torsion angles were 171.62° and 124.46° for **1a** and **4**, respectively. This difference is related to the N3...O hydrogen bond in **1a**, which is absent in **4** and to the presence of the bulky *N*(4)-phenyl substituent in **4**, which causes steric hindrance with the Au1Cl group (See Fig. 2).

In a previously reported work the Au(I)–S bond distance was 2.319 (1) for a complex containing a thiosemicarbazone and a phosphine as ligands [14]. In gold(I) complexes containing two thiosemicarbazones this distance was 2.2825(13) and 2.2818(13) [31]. In complexes (**1a**) and (**4**) the Au(I)–S bond distances are 2.2523(13) and 2.2539(8), respectively. These differences could probably be attributed to the stronger bonds between gold and phosphine [14] or sulfur [31] in the previously reported complexes, compared to the Au–Cl bond in complexes (**1a**) and (**4**).

3.4. Cytotoxicity

HL-60 (acute myeloid leukemia), MCF-7 (human breast adenocarcinoma) and HCT-116 (human colorectal carcinoma) have been

Table 2
Selected bond lengths [Å] for [H₂2Ac4DH]Cl [32], [Au(H₂2Ac4DH)Cl]Cl·H₂O (**1a**), H2Bz4Ph [33] and [Au(H₂2Bz4Ph)Cl]Cl (**4**).

Atoms	[H ₂ 2Ac4DH]Cl	(1a)	H2Bz4Ph	(4)
Au1–S1	–	2.2523(13)	–	2.2539(8)
Au1–Cl1	–	2.2700(13)	–	–
Au1–Cl2	–	–	–	2.2597(8)
S1–C8	1.681(3)	1.712(5)	1.663(2)	1.701(3)
N1–C6	1.335(3)	1.332(6)	1.335(3)	1.329(3)
N1–C2	1.352(3)	1.342(6)	1.343(2)	1.344(3)
N2–C7	1.293(3)	1.283(5)	1.296(2)	1.285(3)
N2–N3	1.358(3)	1.362(5)	1.362(2)	1.354(3)
N3–C8	1.371(3)	1.345(6)	1.360(2)	1.345(3)
N4–C8	1.308(4)	1.303(6)	1.343(3)	1.321(3)
N4–C9	–	–	1.410(2)	1.426(3)
C2–C7	1.480(3)	1.467(6)	1.484(3)	1.480(3)
C7–C9	1.488(4)	1.502(7)	–	–
C7–C15	–	–	1.492(3)	1.490(3)

Table 3
Selected bond angles [°] for [H₂2Ac4DH]Cl [32], [Au(H₂2Ac4DH)Cl]Cl·H₂O (**1a**), H2Bz4Ph [33] and [Au(H₂2Bz4Ph)Cl]Cl (**4**).

Atoms	[H ₂ 2Ac4DH]Cl	(1a)	H2Bz4Ph	(4)
S1–Au1–Cl1	–	173.06(5)	–	–
S1–Au1–Cl2	–	–	–	173.27(3)
C8–S1–Au1	–	109.17(16)	–	107.70(10)
C6–N1–C2	122.7(3)	123.4(4)	118.3(2)	123.3(2)
C7–N2–N3	118.8(2)	119.6(4)	119.4(2)	118.3(2)
C8–N3–N2	119.8(2)	117.7(3)	120.5(2)	120.2(2)
N1–C2–C3	117.6(2)	117.5(4)	121.2(2)	118.0(2)
N1–C2–C7	117.8(2)	118.2(4)	118.1(2)	117.4(2)
C3–C2–C7	124.6(2)	124.3(4)	120.7(2)	124.6(2)
C2–C3–C4	120.4(3)	120.1(5)	119.0(2)	119.5(3)
C5–C4–C3	120.0(3)	119.4(5)	119.4(2)	120.3(3)
C6–C5–C4	118.5(3)	119.3(5)	118.6(2)	118.9(3)
N1–C6–C5	120.8(3)	120.2(5)	123.4(2)	120.0(3)
N2–C7–C2	114.4(2)	114.7(4)	127.5(2)	114.8(2)
N4–C8–N3	117.5(2)	119.6(4)	114.3(2)	118.3(2)
N4–C8–S1	124.7(2)	125.2(4)	128.0(1)	122.0(2)
N3–C8–S1	117.8(2)	115.1(3)	117.7(1)	119.8(2)

employed by the National Cancer Institute (NCI, US) in anticancer drug screen. Approximately one half of the chemotherapeutic drugs currently used by oncologists for cancer treatment were discovered and/or developed at NCI using this strategy. This screening model was rapidly recognized as a rich source of information about the mechanisms of growth inhibition and tumor-cell kill [35]. Jurkat is a cell line derived from human T-cell leukemia which is used to determine the mechanism of differential susceptibility to anti-cancer drugs and radiation.

Leukemia cells are used in screening programs of drug discovery as a predictive model to detect new potential anticancer chemical entities with target on the apoptosis pathway since in these cells apoptosis is very well characterized [36, 37].

Fig. 3 shows the percentages of cell proliferation *versus* control of Jurkat, HL-60, MCF-7 and HCT-116 cell lines in the presence of the thiosemicarbazones, their gold(I) complexes (**1–4**) and HAuCl₄. Since pyridine is a weak base, the proton from the pyridinium ion would be easily released in solution. Hence the active form of compounds (**2–4**) is most likely a neutral gold(I) complex. We used auranofin and cisplatin as positive controls.

According to Fig. 3, in general the thiosemicarbazones and their complexes (**1–4**) demonstrated cytotoxic effect against the tumor cell lines. Jurkat and HL-60 leukemia cells were more sensitive to the compounds than MCF-7 and HCT-116 cells.

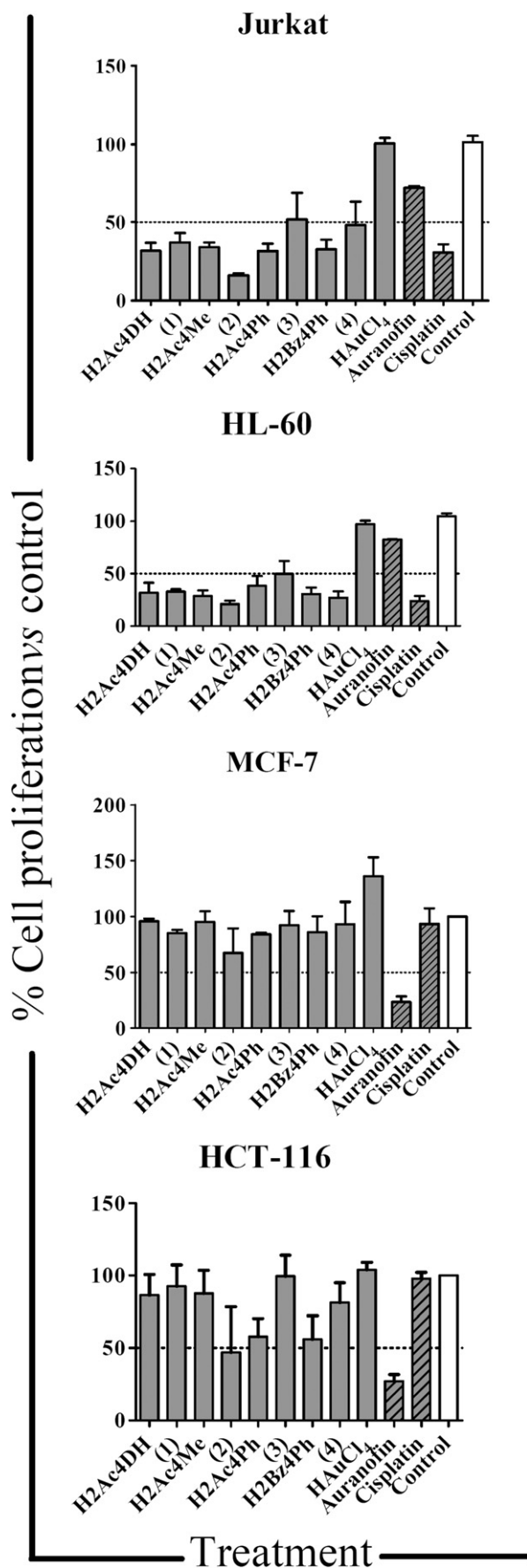
The studied compounds were more cytotoxic than auranofin against Jurkat and HL-60 cells but were in general less active than auranofin against MCF-7 and HCT-116 cells. Many of the studied compounds showed cytotoxicity similar to cisplatin against the investigated leukemia cells. Among all studied compounds complex (**2**) was one of the most cytotoxic. Auranofin revealed to be less cytotoxic to the leukemia

Table 4
Hydrogen bonds [Å and °] for [Au(H₂2Ac4DH)Cl]Cl·H₂O (**1a**) and [Au(H₂2Bz4Ph)Cl]Cl (**4**).

Compound	D–H...A	d(D–H)	d(H...A)	d(D...A)	<(DHA)
(1a)	N1–H1...Cl2A ⁱ	0.86	2.30	3.064(4)	148.7
	N3–H3...O1	0.86	2.03	2.842(5)	157.7
	N4–H4A...Cl2A ⁱ	0.86	2.49	3.277(4)	152.4
	N4–H4B...Cl2	0.86	2.47	3.247(4)	150.4
(4)	O1–H1B...Cl2B ⁱⁱ	0.809(19)	2.53(3)	3.284(5)	155(5)
	O1–H1A...Cl2C ⁱⁱⁱ	0.814(19)	2.51(3)	3.268(4)	157(5)
	N1–H1...Cl1	0.86	2.20	2.988(2)	151.9
	N4–H4A...Cl1	0.86	2.41	3.224(2)	157.1

Symmetry transformations used to generate equivalent atoms:

i = –x + 2, –y + 1, –z + 1, ii = –x + 1, –y + 1, –z + 1, iii = x – 1, y, z.



cells than to the MCF-7 and HCT-116 solid tumor cells. The opposite behavior was observed for cisplatin in the assayed conditions. Interestingly, HAuCl₄ showed no cytotoxic effect against all cell lineages.

The half maximal inhibitory concentration (IC₅₀) was determined for the thiosemicarbazones and complexes (**1–4**) against Jurkat and HL-60 cells and for complex (**2**) against MCF-7 and HCT-116 cells. In order to evaluate the toxicity of the compounds on normal cells, their IC₅₀ was also determined against peripheral blood mononuclear cells (PBMC) (see Table 5). PBMC comprise cells including lymphocytes and monocytes, and are key cells in immune system homeostasis. The immune system can be a target for many chemicals including environmental contaminants and drugs with potential adverse effects on human health. Compounds may affect lymphocytes, which are the primary effectors and regulators of acquired immunity. If the cells are viable (80% or greater) basic functionality can be determined assessing cell proliferation by using mitogens such as phytohemagglutinin (PHA), a plant lectin [38]. In this context, PHA-stimulated PBMC proliferation needs the activation of several metabolic functions involved on immune response. Lymphocytes, in particular T cells, often act as master switches for extensive cascades of immunological processes involved on homeostasis, and on pathological processes [39]. Therefore we used this assay as indicative of the cytotoxicity of compounds as well as of their immunotoxic potential.

According to Table 5, the compounds were more cytotoxic against HL-60 than against Jurkat leukemia cells. H2Ac4Me and H2Ac4Ph were more cytotoxic than auranofin against both leukemia cell lineages. Activity improved on coordination in complexes (**2**) and (**4**) against HL-60 and Jurkat cells. Additionally, **2** proved to be more than fourfold more active against HL-60 cells than the H2Ac4Me ligand. **2** was the most active complex against both cell lines and was the only complex to be more cytotoxic than auranofin against the two leukemia cell lines. Complexes (**2**) and (**4**) were more cytotoxic against HL-60 cells than auranofin. **2** was as active as auranofin against MCF-7 cells but less active than auranofin against HCT-116 cells.

Auranofin was toxic to PBMC cells with a lower IC₅₀ than those determined for its anti-proliferative effect against the four tumor cell lines. Most of the studied compounds were less toxic against PBMC cells than auranofin, except H2Ac4Me and complex (**2**). Toxicity decreases upon coordination in complexes (**3**) and (**4**). H2Ac4DH and complex (**4**) exhibited lower activities against PBMC than against HL-60 cells, thus presenting a good therapeutic index.

In order to investigate the relationship between inhibition of cell proliferation induced by the studied compounds with apoptosis induction we decided to detect the sub-diploid DNA contents in the four tumor cell lines, which indicates DNA fragmentation by apoptosis. Different behaviors were observed (See Fig. 4).

At 10 μM all studied compounds were able to induce more than 50% of DNA fragmentation in HL-60 cells. Complex (**2**) was the compound that induced the least amount of DNA fragmentation, although it was the most cytotoxic. DNA fragmentation with apoptosis induction seems to be one mechanism of action of the studied compounds against HL-60 cells.

The compounds' ability to induce DNA fragmentation was in line with their activities against Jurkat cells, that is, in general the more active compounds the highest amount of DNA fragmentation, indicating that their mechanism of cytotoxic action might involve apoptosis induction.

The percentage of DNA fragmentation was determined only for complex (**2**) and auranofin in MCF-7 and HCT-116 cells. **2** and auranofin showed similar cytotoxic effects on MCF-7 cells and were

Fig. 3. Cytotoxic effect of thiosemicarbazones, their complexes (**1–4**), HAuCl₄, auranofin and cisplatin on Jurkat, HL-60, MCF-7 and HCT-116 cell lines. Cells were treated with compounds (10 μM) for 48 h and the cell proliferation/cell survival was measured by the MTT assay as described in methods. Data are expressed as mean ± SEM of percentage of cell proliferation compared to control (cells treated with DMF 0.1%). Representative data of at least three independent experiments performed in triplicate.

Table 5
Inhibition (IC_{50} , μM) of Jurkat, HL-60, MCF-7 and HCT-116 and PBMC cells proliferation by the thiosemicarbazones, their gold(I) complexes and auranofin. Representative data of at least three independent experiments performed in triplicate.

Compound	IC_{50} (μM) (Confidence interval 95%)				
	Jurkat ^a	HL-60 ^b	MCF-7 ^c	HCT-116 ^d	PBMC ^e
H2Ac4DH (1)	3.502 (0.7896 to 15.53)	2.078 (0.6162 to 7.008)			4.683 (3.115 to 7.042)
H2Ac4Me (2)	50.58 (27.53 to 92.93)	8.615 (6.604 to 11.24)			3.527 (2.618 to 4.751)
H2Ac4Ph (3)	1.422 (0.9881 to 2.047)	0.9251 (0.8120 to 1.054)			0.01250 (0.002454 to 0.06364)
H2Bz4Ph (4)	0.9319 (0.7563 to 1.148)	0.2022 (0.1114 to 0.3669)	1.65 (0.3278 to 8.303)	12.98 (7.236 to 23.27)	0.0002871 (0.00004219 to 0.001953)
Auranofin	1.675 (1.120 to 2.504)	0.07934 (0.03313 to 0.1900)			0.08250 (0.03369 to 0.2021)
	208.4 (56.19 to 773.2)	3.654 (2.036 to 6.560)			0.5222 (0.2494 to 1.093)
	22.99 (19.21 to 25.45)	3.623 (0.9090 to 14.44)			0.7047 (0.3626 to 1.370)
	6.855 (5.057 to 9.294)	1.162 (0.5439 to 2.481)			2.041 (0.4915 to 8.475)
	2.373 (1.323 to 4.258)	1.417 (0.6865 to 2.924)	1.505 (0.5727 to 3.953)	2.674 (1.959 to 3.650)	0.04726 (0.01322 to 0.1690)

^a Jurkat – immortalized line of T lymphocyte cells cell line.

^b HL-60 – acute myeloid leukemia cell line.

^c MCF-7 – human breast adenocarcinoma cell line.

^d HCT-116 – colorectal carcinoma cells.

^e PBMC – peripheral blood mononuclear cells.

both able to induce around 20% DNA fragmentation. Hence DNA fragmentation is probably not the main mechanism of action of these compounds. **2** promoted 100% DNA fragmentation in HCT-116 cells, whereas auranofin promoted around 35% DNA fragmentation. However, auranofin was significantly more active than complex (**2**). The results suggest that DNA fragmentation is probably the main mode of action of complex (**2**) but not of auranofin against HCT-116 cells.

3.5. Studies of interactions with supercoiled plasmid DNA

Since **2** was in general the most cytotoxic complex, its effect on DNA, a possible target for its cytotoxicity, was evaluated. The effect of complex (**2**) on DNA conformation was evaluated by the electrophoretic mobility of the plasmid pGEM-T after association with the complex. At the employed concentration (100 μM) the compound did not significantly alter the electrophoretic mobility of DNA. The

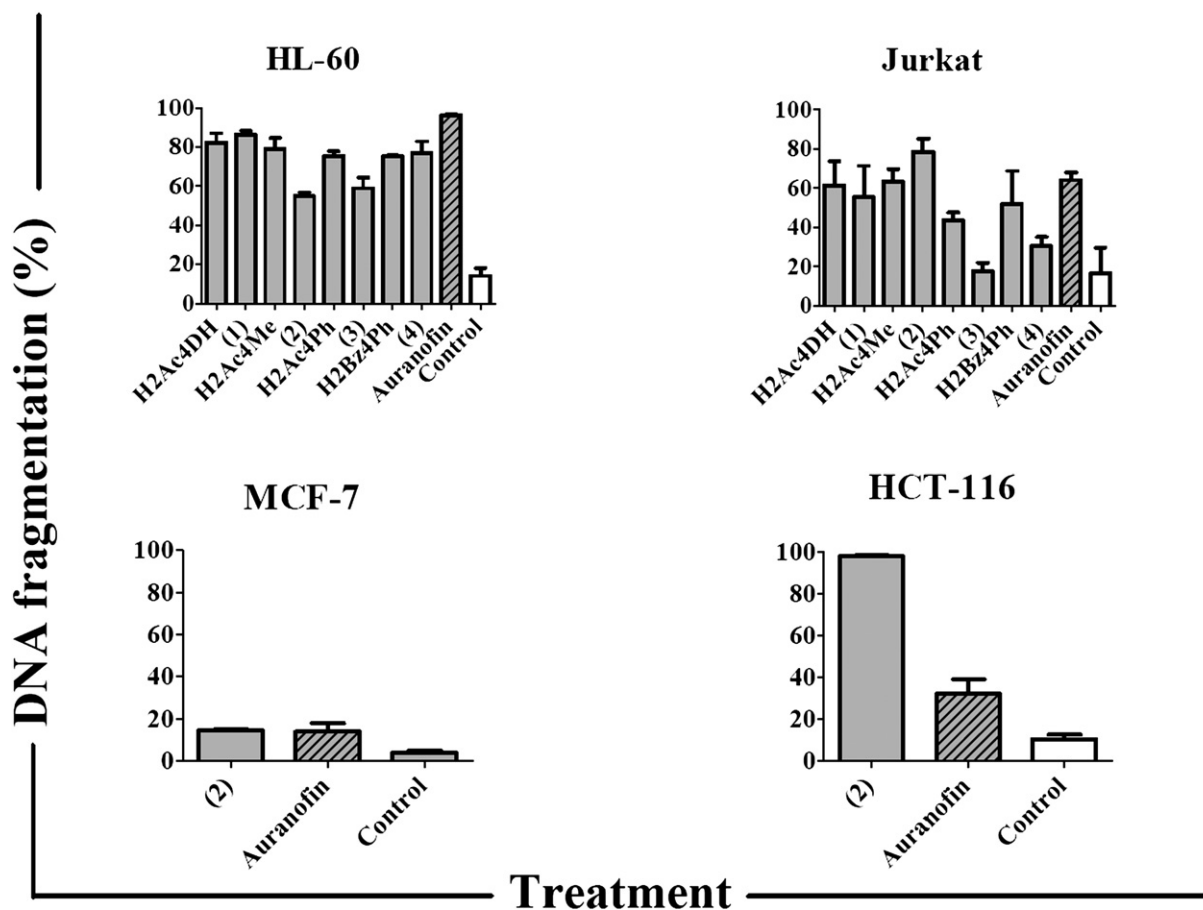


Fig. 4. Percentage of DNA fragmentation in Jurkat, HL-60, MCF-7 and HCT-116 cell lines induced by selected thiosemicarbazones, their gold(I) complexes and auranofin (10 μM). Data are expressed as mean \pm SEM of percentage of DNA fragmentation compared to control (cells treated with DMF 0.1%).

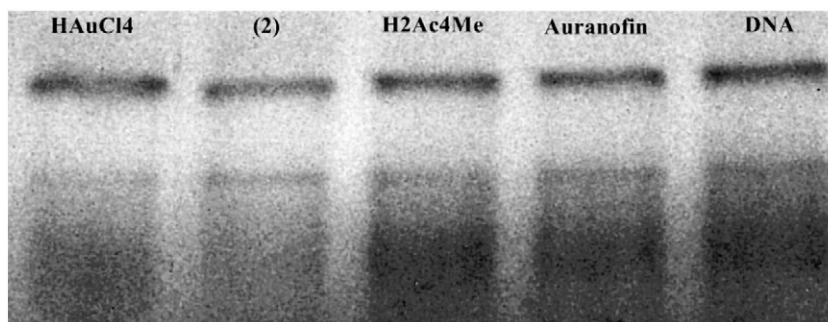


Fig. 5. Agarose (1%) gel electrophoresis pattern of pGEM®-T plasmid DNA incubated at 37 °C for 24 h without (control) or with compounds H2Ac4Me, **2** and HAuCl₄ at 100 μM.

free thiosemicarbazone H2Ac4Me and HAuCl₄ also did not modify the electrophoretic mobility of DNA (See Fig. 5). No plasmid DNA cleavage was observed in the presence of the studied compounds as evidenced by the electrophoretic pattern of DNA which did not undergo significant changes.

Hence, our investigation revealed either that these compounds at 100 μM do not directly interact with the DNA bases or that interaction, if it occurs, does not lead to stable adducts. In addition, the studied compounds did not induce DNA cleavage.

3.6. Inhibition of thioredoxin reductase (TrxR) activity

Inhibition of thioredoxin reductase (TrxR) was considered as another potential mechanism for the anti-proliferative activities of **1–4**. Thus, the *in vitro* inhibitory activities of **2**, H2Ac4Me, HAuCl₄ and auranofin were evaluated using isolated rat liver TrxR, by means of the DTNB reduction assay. This assay makes use of the fact that TrxR reduces the disulfide bonds of DTNB with formation of TNB, which can be detected photometrically.

Complex **(2)** inhibited the enzyme's activity with EC₅₀ = 2.476 μM (95% confidence interval = 2.076 to 2.953 μM) (See Fig. 6) suggesting TrxR as a possible biological target for the cytotoxic action of the complex. The ability of complex **(2)** to inhibit TrxR's activity was compared with those of H2Ac4Me, HAuCl₄ and auranofin at 0.5, 5.0 and 10 μM (Fig. 7), being the last one the same compound concentration used in the anti-proliferative effect assays. We observed that at 0.5 μM, H2Ac4Me and **2** did not inhibit the enzyme's activity, whereas HAuCl₄ and auranofin inhibited 38.2% and 78.9% of TrxR's activity, respectively. At 5.0 μM the percentages of inhibition of TrxR's activity were: 91.5% (**2**), 94.4% (HAuCl₄) and 90.6% (auranofin). At 10.0 μM, **2** inhibited 89.1% of TrxR's activity, while HAuCl₄ and auranofin inhibited 97.3% and 98.9% of TrxR's activity, respectively. H2Ac4Me was unable to inhibit the enzyme's activity in all assayed concentrations.

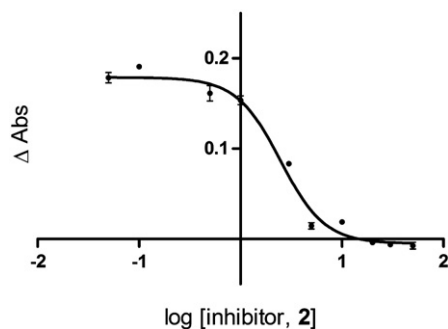


Fig. 6. Inhibitory effect of **2** on TrxR's activity: log[inhibitor, **2**] vs response (absorbance) curve obtained for IC₅₀ determination. Enzyme (0.10 unit) was treated without (control) and with **2** (ten different concentrations in the 0.05–50.0 μM range) for 1 h and TrxR's activity was evaluated by the DTNB assay as described in methods. Representative data of experiments performed in triplicate.

Since not only the gold complex and auranofin but also HAuCl₄ strongly inhibited the enzyme's activity, the inhibitory effect of TrxR may be related to the presence of the gold ion. However, although HAuCl₄ is an inhibitor of TrxR's activity, it did not exhibit cytotoxic effect against HL-60, Jurkat, MCF-7 and HCT-116 tumor cell lines. The hydrophilic character of HAuCl₄ probably hinders its passage through the cell membrane. Unlike HAuCl₄, **2** not only inhibited TrxR's activity but also presented cytotoxic effect, which suggests that the thiosemicarbazone H2Ac4Me, in addition to its own cytotoxic activity, also probably acted as a carrier of the gold ion into the cells. Given the high cytotoxicity of the free ligand, it is possible that the cytotoxic effects of complex **(2)** could be mediated by both gold and the ligand itself following complex disruption as suggested by other authors [40,41]. In this case complex **(2)** would contain two entities to be directed to different targets in one same compound: the thiosemicarbazone, which targets RDR, and gold(I), which targets TrxR.

4. Conclusions

HAuCl₄ showed no cytotoxic effect against all cell lineages. Jurkat and HL-60 leukemia cells were more sensitive to the studied compounds than MCF-7 and HCT-116 cells. The compounds were more cytotoxic than auranofin against Jurkat and HL-60 cells and most of them were less toxic against PBMC cells than auranofin. In some cases activity against both HL-60 and Jurkat cells improved on coordination. **2** was the most cytotoxic complex against all cell lineages and was the only complex to be more cytotoxic than auranofin against the studied leukemia cell lines. **2** was the most active complex but proved to be more toxic to PBMC cells than auranofin. Since complex **(4)** revealed to be more active than its ligand H2Bz4Ph in both leukemia cell lineages, being threefold less toxic than H2Bz4Ph and fortyfold less toxic than auranofin it presents the best therapeutic index.

All studied compounds were able to induce more than 50% DNA fragmentation in HL-60 and Jurkat cells indicating apoptosis induction to be part of their mechanism of cytotoxic action.

2 and auranofin showed similar cytotoxic effects on MCF-7 cells and were both able to induce only around 20% DNA fragmentation, suggesting that DNA fragmentation is probably not the main mechanism of action of these compounds. Complex **(2)** promoted 100% DNA fragmentation in HCT-116 cells, whereas auranofin promoted around 35% DNA fragmentation. Since auranofin was significantly more active than complex **(2)** DNA fragmentation is probably an important mode of action of **2** but not of auranofin against HCT-116 cells.

Complex **(2)** inhibited thioredoxin reductase's (TrxR) activity suggesting TrxR as a possible biological target for its cytotoxic action. At 10.0 μM, **2**, auranofin and HAuCl₄ inhibited 90–99% of TrxR's activity, while H2Ac4Me was unable to inhibit the enzyme's activity in the assayed concentrations. Since not only complex **(2)** and auranofin but also HAuCl₄ strongly inhibited the enzyme's activity, the inhibitory effect of TrxR may be related to the presence of gold. However, although HAuCl₄ is an inhibitor of TrxR's activity, it did

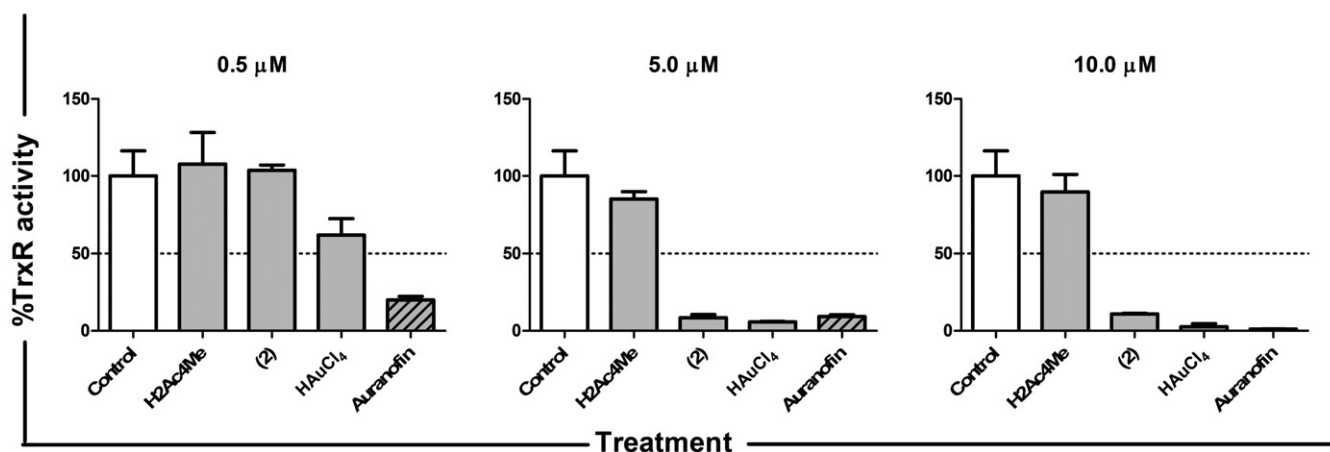


Fig. 7. Inhibitory effect of H2Ac4Me, **2**, HAuCl₄ and auranofin on TrxR. TrxR (0.10 unit) was incubated without (control) and with compounds at 0.5, 5.0 and 10.0 μM for 1 h at 37 °C. TrxR's activity was evaluated by the DTNB assay as described in methods. Representative data of experiments performed in triplicate.

not exhibit cytotoxic effect against the studied tumor cell lines, probably due to its hydrophilic character. Hence, the thiosemicarbazone, besides of its own cytotoxic effect, also probably acted as a carrier of gold ion into the cells.

The literature reports a number of works on gold complexes with TrxR inhibitory properties showing the relevance of this enzyme in the pharmacology of gold-based pharmaceuticals. Due to its antioxidant properties the thioredoxin system prevents cells from oxidative stress, which is a key factor for DNA damage. Overexpression of TrxR has been noticed in numerous tumor cell lines. Moreover, high levels of the substrate thioredoxin have been associated with resistance to cisplatin. Hence TrxR is considered as an attractive target for the development of novel anticancer agents [42]. It has been observed that apoptosis induction by auranofin in Jurkat T cells appeared to be mediated by inhibition of the cytosolic and mitochondrial forms of TrxR and that it was accompanied by an increase in cellular hydrogen peroxide levels [6].

The ability of complex (**2**) to act as an inhibitor of TrxR suggests that this mitochondrial protein is a potential cellular target, and that disruption of mitochondrial function could therefore be a potential mechanism of tumor cell death. Hence although complex (**2**) does not directly interact with DNA, and no plasmid DNA cleavage was observed in the presence of **2**, DNA fragmentation in HL-60, Jurkat and HCT-116 cells in the presence of this complex was probably due to its ability to inhibit TrxR. Inhibition of TrxR may trigger severe mitochondrial deregulation eventually leading to cell apoptosis. Since only 20% of DNA fragmentation was observed in MCF-7 cells in the presence of complex (**2**), TrxR is probably not the main target for the cytotoxic action of **2** in this case.

DNA fragmentation in the presence of auranofin could also be due to its ability to inhibit TrxR's activity.

Since the studied compounds showed a pro-apoptotic profile, they could also be considered as potential "anti-mitochondrial agents" like other gold complexes [42]. To our knowledge this is the first investigation on a gold complex with thiosemicarbazone which behaves as an inhibitor of TrxR.

Our results indicate that further studies of TrxR as a target for thiosemicarbazone's metal complexes should be carried on. The effects of the complexes on mitochondrial membrane potential and permeability, on the accumulation of reactive oxygen species (ROS) in mitochondria and on the expression of proteins associated with inhibition of mitochondrial function should be investigated.

Abbreviations

H2Ac4DH 2-acetylpyridine thiosemicarbazone
H2Ac4Me N(4)-methyl 2-acetylpyridine thiosemicarbazone

H2Ac4Ph N(4)-phenyl 2-acetylpyridine thiosemicarbazone
H2Bz4Ph N(4)-phenyl 2-benzoylpyridine thiosemicarbazone
DMF dimethylformamide
DTNB dithiobisnitrobenzoic acid
NADPH nicotinamide adenine dinucleotide phosphate
PHA phytohemagglutinin
RPMI Roswell Park Memorial Institute
TrxR thioredoxin reductase
TNB 5-thionitrobenzol

Acknowledgments

This work was supported by CNPq and INCT-INOVAR (Proc. CNPq 573.364/2008-6).

Appendix A. Supplementary data

CCDC ID: 827144 and 827145 contain the supplementary crystallographic data for [Au(H₂2Ac4DH)Cl]Cl·H₂O (**1a**) and [Au(H₂2Bz4Ph)Cl]Cl (**4**). These data can be obtained free of charge via <http://www.ccdc.cam.ac.uk/conts/retrieving.html>, or from the Cambridge Crystallographic Data Centre, 12 Union Road, Cambridge CB2 1EZ, UK; fax: (+44) 1223-336-033; or e-mail: deposit@ccdc.cam.ac.uk. Supplementary data to this article can be found online at [doi:10.1016/j.jinorgbio.2011.09.008](https://doi.org/10.1016/j.jinorgbio.2011.09.008).

References

- Barreiro, J.S. Casas, M.D. Couce, A. Sánchez, A. Sánchez-González, J. Sordo, J.M. Varela, E.M.V. López, J. Inorg. Biochem. 104 (2010) 551–559.
- R. Rubbiani, I. Kitanovic, H. Alborzinia, S. Can, A. Kitanovic, L.A. Onambele, M. Stefanopoulou, Y. Geldmacher, W.S. Sheldrick, G. Wolber, A. Prokop, S. Wölfl, I. Ott, J. Med. Chem. 53 (2010) 8608–8618.
- M.P. Rigobello, A. Folda, B. Dani, R. Menabò, G. Scutari, A. Bindoli, Eur. J. Pharmacol. 582 (2008) 26–34.
- F. Magherini, A. Modesti, L. Bini, M. Puglia, I. Landini, S. Nobili, E. Mini, M.A. Cinelli, C. Gabbiani, L. Messori, J. Biol. Inorg. Chem. 15 (2010) 573–582.
- E. Vergara, A. Casini, F. Sorrentino, O. Zava, E. Cerrada, M.P. Rigobello, A. Bindoli, M. Laguna, P.J. Dyson, ChemMedChem 5 (2010) 96–102.
- I. Ott, Coord. Chem. Rev. 253 (2009) 1670–1681.
- H. Beraldo, D. Gambino, Mini Rev. Med. Chem. 4 (2004) 31–39.
- R.A. Finch, M.C. Liu, S.P. Grill, W.C. Rose, R. Loomis, K.M. Vasquez, Y.C. Cheng, A.C. Sartorelli, Biochem. Pharmacol. 59 (2000) 983–991.
- J.A. Lessa, I.C. Mendes, P.R.O. da Silva, M.A. Soares, R.G. dos Santos, N.L. Speziali, N.C. Romeiro, E.J. Barreiro, H. Beraldo, Eur. J. Med. Chem. 45 (2010) 5671–5677.
- A.P. Rebollo, J.D. Ayala, G.M. Lima, N. Marchini, G. Bombieri, C.L. Zani, E.M. Souza-Fagundes, H. Beraldo, Eur. J. Med. Chem. 40 (2005) 467–472.
- I.C. Mendes, M.A. Soares, R.G. dos Santos, C. Pinheiro, H. Beraldo, Eur. J. Med. Chem. 44 (2009) 1870–1877.
- D.C. Reis, M.C.X. Pinto, E.M. Souza-Fagundes, S.M.S.V. Wardell, J.L. Wardell, H. Beraldo, Eur. J. Med. Chem. 45 (2010) 3904–3910.
- K.S.O. Ferraz, G.M.M. Cardoso, C.M. Bertollo, E.M. Souza-Fagundes, N. Speziali, C.L. Zani, I.C. Mendes, M.A. Gomes, H. Beraldo, Polyhedron 30 (2011) 315–321.

- [14] J.S. Casas, E.E. Castellano, M.D. Couce, J. Ellena, A. Sánchez, J. Sordo, C. Taboada, *J. Inorg. Biochem.* 100 (2006) 1858–1860.
- [15] U. Abram, K. Ortner, R. Gust, K. Sommer, *J. Chem. Soc., Dalton Trans.* (2000) 735–744.
- [16] A.P. Rebolledo, G.M. Lima, N.L. Speziali, O.E. Piro, E.E. Castellano, J.D. Ardisson, H. Beraldo, *J. Organomet. Chem.* 691 (2006) 3919–3930.
- [17] CRYCALISPRO, Oxford Diffraction Ltd., Version 1.171.33.55 (release 05-01-2010 CrysAlis171.NET).
- [18] CRYCALISPRO, Oxford Diffraction Ltd., Version 1.171.33.36 (release 16-03-2009 CrysAlis171.NET).
- [19] G.M. Sheldrick, *Acta Crystallogr. A* 64 (2008) 112–122.
- [20] G. Gazzinelli, N. Katz, R.S. Rocha, D.G. Colley, *J. Immunol.* 130 (1983) 2891–2895.
- [21] T.J. Mosmann, *Immunol. Methods* 65 (1983) 55–63.
- [22] E. Ulukaya, M. Colakogullari, E. Wood, *J. Exp. Chem.* 50 (2004) 43–50.
- [23] I. Nicoletti, G. Migliorati, M.C. Pagliacci, F. Grignani, C. Riccardi, *J. Immunol. Methods* 139 (1991) 271–279.
- [24] I. Ott, X. Qian, Y. Xu, D.H.W. Vlecken, I.J. Marques, D. Kubutat, J. Will, W.S. Sheldrick, P. Jesse, A. Prokop, C.P.J. Bagowski, *J. Med. Chem.* 52 (2009) 763–770.
- [25] I.G. Santos, A. Hagenbach, U. Abram, *Dalton Trans.* (2004) 677–682.
- [26] R.H.U. Borges, E. Paniago, H. Beraldo, *J. Inorg. Biochem.* 65 (1997) 267–275.
- [27] A. Castiñeiras, R. Pedrido, G. Pérez-Alonso, *Eur. J. Inorg. Chem.* (2008) 5106–5111.
- [28] B. Chenon, C. Sandorfy, *Can. J. Chem.* 36 (1958) 1181–1206.
- [29] A. Garza-Ortiz, J. Dulk, J. Brouwer, H. Kooijman, A.L. Spek, J. Reedijk, *J. Inorg. Biochem.* 101 (2007) 1922–1930.
- [30] T.S. Lobana, S. Khanna, R.J. Butcher, *Inorg. Chem. Commun.* 11 (2008) 1433–1435.
- [31] S.D. Khanye, N.B. Báthori, G.S. Smith, K. Chibale, *Dalton Trans.* 39 (2010) 2697–2700.
- [32] S. Abram, U. Abram, Ulrich, *Acta Crystallogr. C* 53 (1997) 360–362.
- [33] A.P. Rebolledo, G.M. de Lima, L.N. Gambi, N.L. Speziali, D.F. Maia, C.B. Pinheiro, J.D. Ardisson, M.E. Cortes, H. Beraldo, *Appl. Organomet. Chem.* 17 (2003) 945–951.
- [34] P.J. Bonasia, D.E. Cindelberger, J. Arnold, *Inorg. Chem.* 32 (1993) 5126–5131.
- [35] R.H. Shoemaker, *Nat. Rev. Cancer* 6 (2006) 813–823.
- [36] K.A. Tacka, J.C. Dabrowiak, J. Goodisman, H.S. Penefsky, A.K. Souid, *Chem. Res. Toxicol.* 17 (2004) 1102–1111.
- [37] M. Monga, E.A. Sausville, *Leukemia* 16 (2002) 520–526.
- [38] M. Carfi, A. Gennari, I. Malerba, E. Corsini, M. Pallardy, R. Pieters, H. Van Loveren, H.W. Vohr, T. Hartung, L. Gribaldo, *Toxicology* 229 (2007) 11–22.
- [39] F.F. Mahmoud, D.D. Haines, H.T. Abul, A.T. Abal, B.O. Onadeko, J.A. Wise, *J. Pharmacol. Sci.* 94 (2004) 129–136.
- [40] A.N. Wein, A.T. Stockhausen, K.I. Hardcastle, M.R. Saadein, S. Peng, D. Wang, D.M. Shin, Z. Chen, J.F. Eichler, *J. Inorg. Biochem.* 105 (2011) 663–668.
- [41] L. Messori, F. Abbate, G. Marcon, P. Orioli, M. Fontani, E. Mini, T. Mazzei, S. Carotti, T. O'Connell, P. Zanello, *J. Med. Chem.* 43 (2000) 3541–3548.
- [42] A. Bindoli, M.P. Rigobello, G. Scutari, C. Gabbiani, A. Casini, L. Messori, *Coord. Chem. Rev.* 253 (2009) 1692–1707.